



CORROSION DAMAGE FOR PRESTRESSED CONCRETE BRIDGE GIRDERS

YANAKA MAKOTO,

Structural Engineer, Japan Highway Public Corporation, Nagoya, Japan

NOWAK ANDRZEJ S., *nowak@auburn.edu*

Professor and Chair of Civil Engineering, Auburn University, Auburn, USA

GHASEMI SEYED HOOMAN

Post-Doctoral Research Associate of Civil Engineering, Auburn University, Auburn, USA

Abstract: The deterioration process includes three stages: diffusion of chlorides, corrosion of steel strands, and cracking/spalling of concrete. The time to initiation of corrosion depends on concrete cover depth, quality of protective coating (if any), and diffusion coefficient. Occurrence of cracks can be very important, as it facilitates the penetration of aggressive chemicals (salt). The diffusion coefficient can be significantly larger for cracked sections (areas) than for intact concrete. For the cracked section under service load, it is taken as an average value with regard to time and area. A 2-D and 3-D models are developed for prediction of the chloride concentration at the surface of reinforcement. The probability of the initiation of corrosion is calculated for representative design cases. Recommendations are formulated for design of prestressed concrete bridge girders, including allowable tensile stress and cover depth for various conditions (i.e. level of exposure to marine environment).

1. Introduction

New generation of reliability-based design codes for buildings and bridges have been developed in various countries. Load and resistance parameters are random in nature and, therefore, reliability can be used as a rational measure of structural performance. Probabilistic approach makes it possible to quantify the level of uncertainty. The design parameters (load and resistance factors) are determined in the calibration process. So far, most of the code calibration effort was directed to the development of the ultimate load criteria. However, the serviceability limit states (SLS) often govern in the design of bridges. Therefore, there is a need for the reliability-based calibration of SLS. The allowable tensile stress after prestressing losses is directly related to cracking due to the applied loads and it is indirectly related to steel corrosion in concrete.

When chloride concentration reaches a threshold level of the chloride concentration for the initiation of corrosion at the surface of reinforcement, corrosion can start. As time passes, steel induces tensile stress in the surrounding concrete since products of corrosion have half of the density of sound steel. Consequently, this change of density can cause cracks on the concrete surface. After cracking due to corrosion of steel occurs, the rate of corrosion becomes much faster because sufficient oxygen can be supplied through the crack [Williamson and et.al 2009]. It is well known that cracks can accelerate corrosion. In the past, the design codes specified an allowable crack width, determined by engineering judgment, rather than by analysis of the corrosion effect. New research showed that corrosion was not necessarily correlated with the surface width of cracks. Therefore, in the new generation of codes, including AASHTO LRFD [2015] and ACI 318 [2014], crack width limit has been replaced with allowable stress in

the tensile reinforcement and/or minimum spacing of tensile reinforcement. However, the new requirements are still indirectly based on the allowable crack width.

A considerable research effort has been focused on investigation of the relationship between the time to initiation of corrosion, the rate of corrosion, and the crack width, the latter being unchanged during the experiments [e.g., Otsuki and et.al 2010; Ostermiski and Shieβl 2012; Arya and et.al 2014; TakewakA et al. 2003]. In reality, however, crack can be opened and closed depending on loads; therefore, it is necessary to consider this opening and closing effect. The rate of crack occurrence depends on the depth of concrete cover, the type of reinforcement, and the nature of live load. In the above quoted literature, the problem was considered from a deterministic rather than reliability point of view.

Spatial time-dependent reliability analysis of corroding pretensioned prestressed concrete bridge girders was evaluated by Darmawan and Stewart [2007], and Thoft-Christensen [2008] investigated the deterioration steps and reliability of concrete structures.

Therefore, the purpose of this study is to determine the initiation period for prestressed concrete girder bridges, which is the time needed by the chlorides on the surface of concrete to reach the prestressing steel and initiate the corrosion. The major parameters considered include threshold level of chloride concentration, diffusion coefficient, cover depth, concrete strength (compression and tension), and level of exposure to marine environment. Heavy trucks may cause cracking of concrete. Therefore, the analysis is performed for two cases: uncracked concrete, and cracked concrete.

2. Corrosion of Steel in Concrete

The life cycle model of a reinforced concrete structure can be divided into three distinct phases: diffusion, corrosion, and deterioration. The first phase, diffusion, is defined as the period when aggressive materials penetrate and reach the corrosion threshold level on the steel surface. The second phase, corrosion, is defined as a period of time from the initiation of corrosion to first cracking caused by steel expansion. The third phase, deterioration, describes the time to reach a damage level that requires a repair or rehabilitation since at the third phase, the rate of deterioration becomes much faster [Williamson and et.al 2009].

Chloride-Induced Corrosion

It is well known that the presence of chloride ions in reinforced concrete can cause corrosion if exposed to sufficient oxygen and water. Chloride-induced corrosion is the most prevalent and damaging cause of corrosion of steel reinforcement. In practice, there is a threshold level of the chloride concentration that must be exceeded before corrosion occurs. Chlorides originate from four sources: (1) calcium chlorides added to the mix as an accelerator, (2) sodium chloride ingress from exposure to a marine environment, (3) sodium chloride ingress from dissolved salt used as deicing salt on roads and bridges, and (4) sodium chlorides contained within the concrete aggregate.

Diffusion of Chloride Ions in Concrete

Chloride diffusion is a specific case of scalar field problems that are encountered in almost all branches of engineering and physics. Most of them can be viewed as special forms of the general Helmholtz Equation given by

$$\frac{\partial}{\partial x} \left(k_x \frac{\partial \phi}{\partial x} \right) + \frac{\partial}{\partial y} \left(k_y \frac{\partial \phi}{\partial y} \right) + \frac{\partial}{\partial z} \left(k_z \frac{\partial \phi}{\partial z} \right) + Q = c\rho \frac{\partial \phi}{\partial t} \quad (1)$$

where: k_x , k_y , and k_z = ion conductivity in x , y , and z – direction, respectively, Q = ion supply, c = specific value of ion content, ρ = density of concrete, t = time, and $\varphi(xyz)$ = the field variable to be solved.

For a constant surface concentration and a one-dimensional problem, under the conditions, $C(0, t) = C_0$ and $C_i = 0$, Eq. 1 yields

$$C(x, t) = C_0(1 - \operatorname{erf}(\eta)) = C_0 \left(1 - \operatorname{erf} \left[\frac{x}{2\sqrt{D_c t}} \right] \right) \quad (2)$$

where: $C(x, t)$ = ion concentration at the surface of steel at time t , x = cover depth, C_0 = ion concentration at the surface of concrete, D_c = a diffusion coefficient and $\operatorname{erf}(\eta)$ = the Gaussian error function. D_c can be expressed as $D_c = k/\rho c$ [Incropera and Dewitt 1996].

Diffusion Coefficient

Diffusion coefficient, D_c , is an important property which measures the ability of material to conduct ions relative to its ability to store ions. Materials with large D_c will respond quickly to changes in their ion concentration, while materials with small D_c will respond more slowly, taking longer to reach a new equilibrium condition [Incropera and Dewitt 1996]. Although there are several studies in which the time-dependent effect, the water cement ratio, and the temperature effect are considered [e.g. Samson and Marchand 2009; Weng et al. 2006; Tanaka et al. 2001], the diffusion coefficient is a random variable rather than a deterministic value because of the nature of concrete. For example, Stewart [1997] assumed that diffusion coefficient, is lognormally distributed with the mean value of $2.0 \cdot 10^{-8}$ cm²/s and coefficient of variation, $V = 0.75$. In the present study, the statistical parameters shown in Table 1 are used for the diffusion coefficient. The values are obtained from the test data of concrete cores taken from existing bridges [Tanaka et al. 2001].

Table 1. Statistical Data for Diffusion Coefficient

Concrete strength	Number of samples	Mean (cm ² /s)	C.O.V.	Distribution
40 Mpa	47	1.2.E-08	1.31	Lognormal
50 Mpa	17	3.3.E-09	1.00	Lognormal

3. Crack Width and Diffusion Coefficient

There have been many studies of the relationship between crack width and corrosion rate. Although a larger crack width can result in an increased corrosion rate, several researchers found a weak relationship between crack width and corrosion rate. Several design codes limit the crack width to control the rate of corrosion, while other codes do not. The current ACI code [2014] limits the spacing of reinforcement closest to concrete surface since crack width in structures can vary. The predicted crack width at the surface of concrete can be determined based on the study by the Gergely and Lutz [1968]:

$$W_{\max} = 0.76 \cdot 10^{-3} \cdot \beta \cdot f_s \cdot \sqrt[3]{d_c \cdot A_b} \quad (3)$$

where: f_s = service load stress in reinforcement, β = the distance from the neutral axis to the bottom fiber, divided by the distance to the reinforcement, d_c = the distance from

the extreme tension fiber to the center of the reinforcing bar located closest to it, and A_b = the effective tension area of concrete surrounding the tension reinforcement, and having the same centroid as that reinforcement, divided by the number of bars or wires. It should be noted that Eq. 3 is given in inches (1 inch = 25.4 mm).

Effect of Crack Width on Diffusivity of Chloride Ions

In concrete, cracks can be generated due to various causes, such as drying shrinkage or load effect. These cracks are likely to influence the diffusivity of chloride ions into concrete. Takewaka et al. [2003] experimentally derived the relationship between crack width and diffusion coefficient of a cracked section as shown in the following equations,

$$D_c = 1.2 \times 10^{-8} \exp\{136.33 w\} \text{ for } (0 \leq w \leq 0.1 \text{ mm}) \text{ (40 MPa – concrete)} \quad (4)$$

$$D_c = 3.3 \times 10^{-9} \exp\{149.24 w\} \text{ for } (0 \leq w \leq 0.1 \text{ mm}) \text{ (50 MPa – concrete)} \quad (5)$$

$$D_c = 1.2 \times 10^{-8} \text{ for } (0.1 \leq w) \quad (6)$$

where D_c = the diffusion coefficient (cm²/sec) and w is the crack width (mm).

In general, the diffusion coefficient of a cracked concrete is much larger than that of sound concrete. The diffusion coefficient of sound concrete is less than 1.0 cm²/year, while that of the cracked concrete may be two to three orders larger.

4. Statistical Data for Loads and Resistances

The statistical parameters of the dead load are specified by Nowak and Collins [2013]. The static and dynamic live load model was developed in conjunction with the development of the AASHTO LRFD code [Nowak 1999], based on the truck survey data.

The materials used in prestressed concrete bridge girders are prestressing and reinforcing steel and concrete. The randomness of the behavior of these materials arises due to the variability in material strength, accuracy of the strength prediction model, and the fabrication. The statistical data and the distribution of resistance are taken from Nowak and Collins [2013] and Nowak and Rackoczy [2012]. MacGregor [1997] indicates that 10% of the measured crack widths exceed 1.5 times the value given by Eq. 6, while 2% of the measured crack widths are less than 0.5 times the calculated width. Assuming that the distribution is a normal random variable, the bias factor and the coefficient of the variation of crack width are 1.116 and 0.269, respectively.

5. Design of Prestressed Concrete Bridge Girders

In order to cover a wide range of different types of prestressed concrete bridge girders, the analysis is performed for three different spans, three values of the allowable tensile stress, two cover depths, and two values of the concrete compressive strength, as summarized in Table 2. Girder spacing and slab thickness are assumed to be 2.4 m and 225 mm, respectively. All designs are based on only the allowable tensile stress, which usually governs the design of prestressed concrete bridge girders. The total number of considered design cases is 36.

Note that in the present study, the allowable tensile stress is defined using parameter K ,

$$\text{allowable tensile stress} = K \sqrt{f'_c} \text{ (MPa)} \quad (8)$$

where: $K = 0, 0.25, \text{ and } 0.50$. In further discussion, the considered three allowable stress values are denoted by corresponding value of K .

Table 2. Design Parameters

Parameters	Values of parameters used in this study
Span	12 m, 18 m, 24 m
Allowable tensile stress	$0 \text{ MPa}, 0.25\sqrt{f'_c} \text{ MPa}, 0.5\sqrt{f'_c} \text{ MPa}$
Cover depth	50 mm, 75 mm
Concrete compressive strength	40 MPa, 50 MPa

Cracking Moment, Decompression Moment, Stress in Prestressing Strands

The cumulative distribution functions (CDF) were obtained for the cracking moment, M_{cr} , decompression moment, M_{dc} , stress in prestressing steel, and stress at the bottom of girder, using a specially developed computer procedure, with Monte Carlo simulations and Al-Zaid’s algorithm (1986). The results are shown in figure 1 for 75 years after the beginning of the service life of the bridge. The CDFs are plotted on the normal probability paper [Nowak and Collins 2013].

The considered structure consists of prestressed precast concrete girders and reinforced concrete slab (cast in place). Figure 2 shows the mean values of the decompression moment, M_{dc} , and cracking moment, M_{cr} . It is assumed that the slab is cast-in-place using unshored construction 180 days after casting of the girders. Therefore, there is a discontinuity corresponding to 180 days in Figure 2. In addition, the nominal values of M_{dc} , and M_{cr} obtained by the elastic analysis are shown as straight lines in figure 2 representing the mean values of stress in prestressing steel.

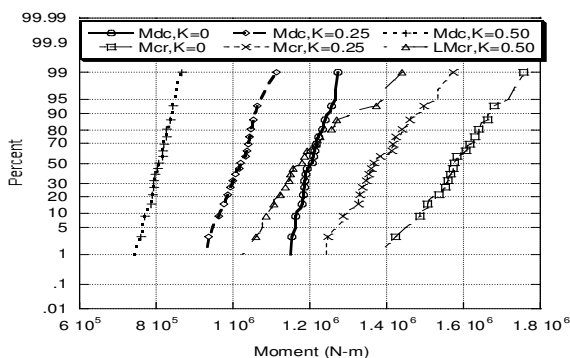


Fig. 1. Distribution of Decompression Moment and Cracking Moment (Span = 12 m, 40 MPa, Cover = 50 mm, After 75 years)

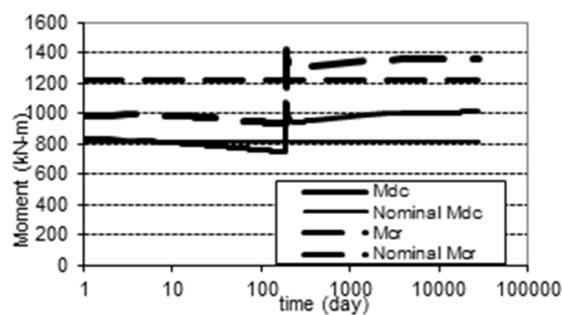


Fig. 2. Decompression Moment and Cracking Moment versus Service Time (40 MPa, Span = 12 m, $K = 0.25$, Cover = 50 mm)

As presented in Figure 1, both the decompression moment and the cracking moment depend on the allowable tensile stress (K value). In addition, the decompression moment and the cracking moment can be assumed to follow normal distributions. From Figure 2, after casting the slab, there is no significant change in the decompression moment and the cracking moment. This tendency is also consistent with Al-Zaid’s calculation (1988).

Time to the First Cracking

The first cracking occurs when the applied load exceeds the cracking moment, M_{cr} . However, after the first cracking occurs, concrete loses its tensile strength and consequently cracking occurs whenever the applied load exceeds the decompression moment, M_{dc} .

Figure reveals the relationship between the ratio between the decompression moment and the service moment, the span, and the concrete strength. In figure Fig, the type of the AASHTO type girder used for the design is indicated (e.g. Type II). As illustrated in the Figure 3, the higher compressive strength of concrete results in a smaller ratio between the decompression moment and the service moment. In addition, it can be observed that the longer girders tend to make the ratio greater. In order to explain this tendency, a noncomposite case is considered because of simplicity. The design formula for the allowable tensile stress can be expressed as follows [Naaman 2004]:

$$\frac{F}{A_c} + \frac{Fe}{S_b} - \frac{M_{serv.}}{S_b} \geq \sigma_{ts} \quad (9)$$

where: F = effective prestressing force, A_c = area of a girder, e = eccentricity of the prestressing force, S_b = section modulus with respect to the bottom fiber, $M_{serv.}$ = service moment, and σ_{ts} = the allowable tensile stress. From Eq. 9, the following inequation can be obtained.

$$F \left(\frac{S_b}{A_c} + e \right) - \sigma_{ts} S_b = M_{dc} - \sigma_{ts} S_b \geq M_{serv.} \quad (10)$$

since $M_{dc} = F * (S_b/A_c + e)$. From Eq. 10, the ratio between the decompression moment, M_{dc} , and the service moment, $M_{serv.}$ can be obtained as follows:

$$\frac{M_{dc}}{M_{serv.}} \geq 1 + \frac{\sigma_{ts} S_b}{M_{serv.}} \quad (11)$$

Note σ_{ts} is a negative value. From Eq. 11, for a given section, the ratio between M_{dc} and $M_{serv.}$ increases as span length increases since $M_{serv.}$ also increases (i.e., the second term of the right hand side approaches negative zero from a negative value when span length increases). This is the reason for the tendency which can be seen in Figure Fig7.

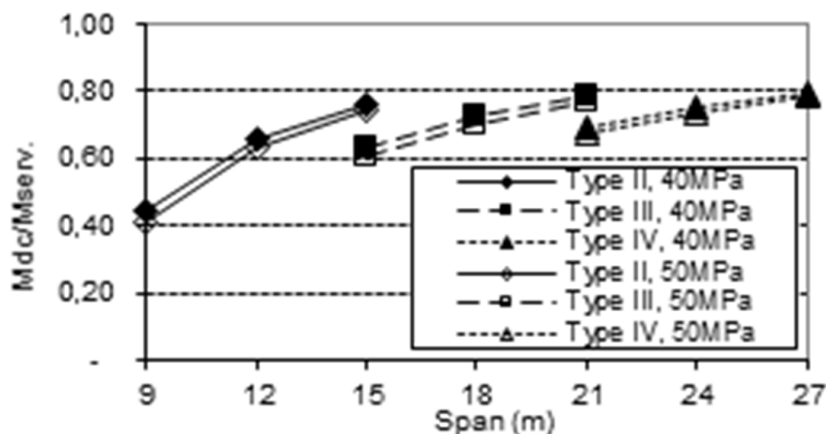


Fig. 3. The Ratio between the Decompression Moment and the Service Moment versus Span ($K = 0.50$, Cover = 50 mm)

6. Diffusion Coefficient of the Cracked Area

The diffusion coefficient of the cracked area, which is averaged in respect of time and area, can be obtained using Monte Carlo simulations. For crack opening time, which is necessary to take average of the diffusion coefficient, the mean value of the crack opening time at the bottom of the girder is used. A 1 – mm cracked area is used to obtain the average diffusion coefficient. Figure 4 shows the relationship between the averaged diffusion coefficient of the cracked area and crack depth. The averaged diffusion coefficient of the cracked area is calculated for the beginning of the bridge service, and after 3 years, 6 years, 15 years, and 75 years. The crack depth is taken from the bottom of the girder. Figure 5 shows the relationship between the averaged diffusion coefficient of the cracked area at the bottom of the girder and service time.

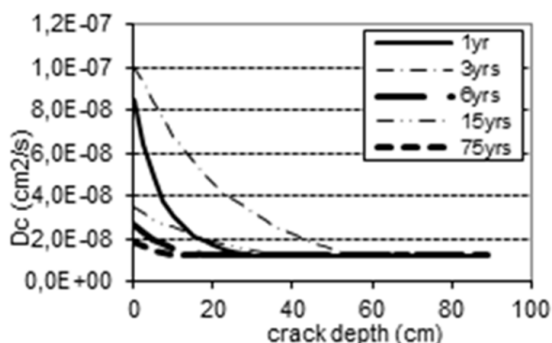


Fig. 4. Averaged Diffusion Coefficient (40 MPa, Span = 12 m, $K = 0.25$, cover = 50 mm, ADTT = 5000)

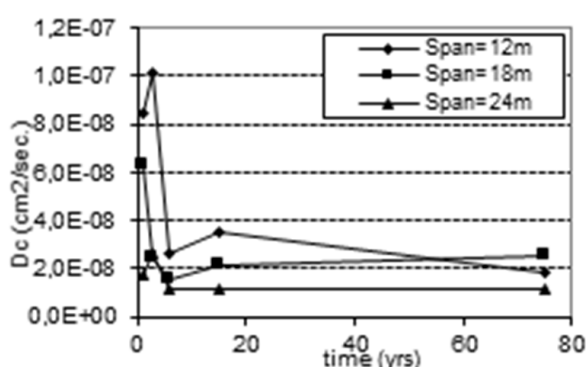


Fig. 5. Time-Dependent Averaged Diffusion Coefficient versus Service Time (40 MPa, $K = 0.25$, Cover = 50 mm, ADTT = 5000)

As expected, the diffusion coefficient of the cracked area decreases as crack depth (i.e. the distance from the bottom of a girder) increases since crack width and crack opening time also decreases. From figure 5, after 3 years, it appears that the change in the averaged diffusion coefficient becomes relatively small.

7. Probability of Corrosion

Using the probabilistic data of the chloride concentration obtained by FEA with Monte Carlo method, the initiation of corrosion can be evaluated. The probabilities are expressed as the probabilities of the initiation of corrosion within 75 years. The probabilities of the two-dimensional models and the three-dimensional models are provided in and figure, respectively. The horizontal axis of figure indicates the distance from the center line of a girder.

Table 3. Probability of Initiation of Corrosion ($C_0 = 0.00369 \text{ g/cm}^3$)

		12 m			18 m			24 m		
Concrete	Cover	$K = 0.00$	$K = 0.25$	$K = 0.50$	$K = 0.00$	$K = 0.25$	$K = 0.50$	$K = 0.00$	$K = 0.25$	$K = 0.50$
40 MPa	50 mm	1.00	1.00	1.00	1.00	1.00	1.00	1.00	1.00	1.00
	75 mm	0.66	0.76	1.00	0.66	0.66	1.00	0.65	0.65	1.00
50 MPa	50 mm	0.39	0.80	1.00	0.39	0.37	1.00	0.38	0.47	1.00
	75 mm	0.03	0.10	1.00	0.02	0.06	1.00	0.06	0.07	1.00

Table 4. Probability of Initiation of Corrosion ($C_0 = 0.00212 \text{ g/cm}^3$)

Concrete	Cover	12 m			18 m			24 m		
		K = 0.00	K = 0.25	K = 0.50	K = 0.00	K = 0.25	K = 0.50	K = 0.00	K = 0.25	K = 0.50
40 MPa	50 mm	0.61	0.65	1.00	0.55	0.65	0.96	0.56	0.59	0.73
	75 mm	0.14	0.14	1.00	0.15	0.15	0.84	0.13	0.13	0.40
50 MPa	50 mm	0.09	0.17	1.00	0.07	0.07	0.97	0.11	0.08	0.84
	75 mm	0.01	0.02	1.00	0.02	0.03	0.82	0.01	0.03	0.96

Table 5. Probability of Initiation of Corrosion ($C_0 = 0.00122 \text{ g/cm}^3$)

Concrete	Cover	12 m			18 m			24 m		
		K = 0.00	K = 0.25	K = 0.50	K = 0.00	K = 0.25	K = 0.50	K = 0.00	K = 0.25	K = 0.50
40 MPa	50 mm	0.08	0.11	0.49	0.13	0.09	0.22	0.13	0.07	0.11
	75 mm	0.03	0.05	0.60	0.04	0.04	0.14	0.02	0.02	0.02
50 MPa	50 mm	0.01	0.05	0.57	0.02	0.03	0.23	0.01	0.01	0.10
	75 mm	0.00	0.00	0.90	0.01	0.00	0.07	0.00	0.00	0.17

As can be seen, the allowable tensile strength, concrete strength, and cover depth affect the probability of the initiation of corrosion. Assuming that the allowable probability of corrosion is 0.159, which corresponds to 1.0 in the reliability index, all design cases can be evaluated in terms of the probability of corrosion, and the cases which do not satisfy the allowable probability of corrosion are hatched in the Tables 3–5. The probability of corrosion tends to decrease as the cover increases and the allowable tensile stress decreases. Higher concrete strength can also achieve a smaller probability of corrosion since higher strength concrete can achieve smaller diffusion coefficient of sound concrete.

In addition, the three-dimensional effect is also recognized (fig. 6). Thus it might be necessary to consider the three-dimensional effect for the diffusion of the chloride ions. It can be safely said that cover depth from the side surface needs to exceed 75 mm.

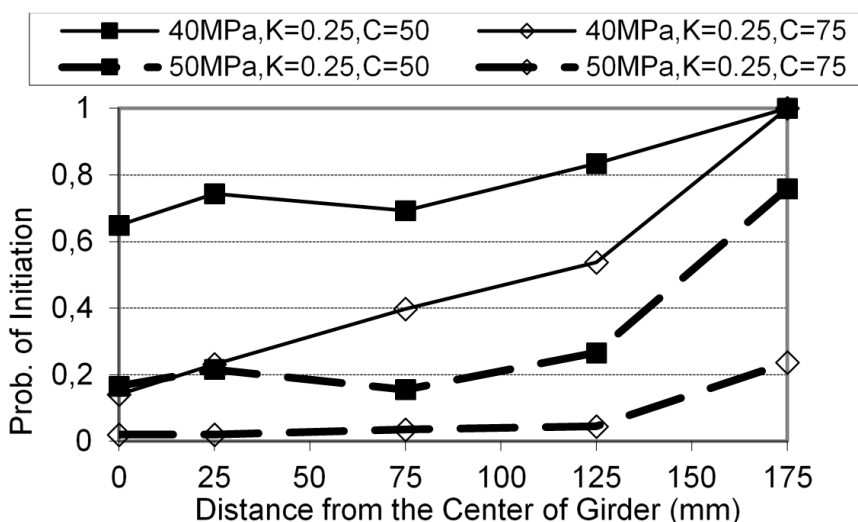


Fig. 6. Probability of Initiation of Corrosion (3-Dimensional, $C_0 = 0.00212 \text{ g/cm}^3$, $K = 0.25$)

8. Conclusion

The study deals with the development of a model for the chloride diffusion time for prestressed concrete AASHTO type bridge girders. In order to model the opening and closing motion of cracks due to the applied loads, the diffusion coefficient of the cracked area, which is averaged with regard to time and area, is used.

In order to approach the problem, cracking due to the applied loads must initially be considered. The averaged diffusion coefficients of the cracked area can be obtained by utilizing the developed model that can take into account the opening and closing motion of cracks.

Using the diffusion coefficient of the cracked area, finite element analysis with Monte Carlo method is carried out to obtain the chloride concentration at the surface of reinforcement. The results are utilized to obtain the probability of the initiation of corrosion. From the probability of the initiation of corrosion, the design recommendations for various environments can be obtained.

Several conclusions can be derived from the present study. These conclusions are summarized as follows:

- Increase of the allowable tensile stress results in the increase of the probability of cracking. Consequently, the diffusion coefficient of the cracked area increases as the allowable tensile stress increases. In addition, it is possible to obtain the probability of cracking from the ratio between the decompression moment and the service moment.
- In general, the case with an allowable tensile stress = $0.25\sqrt{f'_c}$ MPa shows little difference from the case with a zero-allowable tensile stress in terms of the average diffusion coefficient of the cracked area. While in the case with an allowable tensile stress = $0.50\sqrt{f'_c}$ MPa, the diffusion coefficient of the cracked area is much larger than that of sound concrete.
- Cracking due to corrosion of the reinforcement might have a relatively small effect on the total time to the visibility of corrosion since cracking due to corrosion can be observed approximately two years after the initiation of corrosion. Therefore, the time to the initiation of corrosion or the probability of initiation of corrosion during service life is more important than the time to the cracking due to corrosion for practical situations.
- Assuming the allowable probability of the initiation of corrosion, the design recommendations, such as concrete strength, concrete cover, and the allowable tensile stress, for various environments can be developed.

References

1. AASHTO, (2015), AASHTO LRFD Bridge Design specifications, American Association of State Highway and Transportation Officials, 7th Edition, Washington, D.C.
2. ACI, (2014), Building code requirements for structural concrete (ACI 318-14) and Commentary, American concrete institute, Michigan.
3. Al-Zaid R. Z., Naaman A. E., Nowak A. S., (1988), "Partially Prestressed Composite Beams under Sustained and Cyclic Loads", Journal of Structural Engineering, Vol.114, No.2, pp.269–291, February.
4. Arya C., Vassie P., Bioubakhsh S., (2014), "Modeling chloride penetration in concrete subjected to cycle wetting and drying", Magazine of Concrete Research, Vol.66, No.7, pp.364–376.
5. Darmawan M. S., Stewart M. G., (2007), "Spatial time-dependent reliability analysis of corroding pretensioned prestressed concrete bridge girders", Structural Safety, Vol.29, No.1, pp.16–31.
6. Gergely P., and Lutz L. A., (1968), "Maximum Crack Width in Reinforced Concrete Flexural Members," Causes, Mechanism, and Control of Cracking in Concrete, SP-20, American Concrete Institute, Detroit.

7. Hwang E. S., Nguyen S. H., Nguyen Q. H, (2014), "Development of Serviceability Limit State Design Criteria for Stress in Prestressed Concrete Girders", *KSCE Journal*, Vol.18, No.7, pp.2143–2152.
8. Incropera F. P., DeWitt D. P., (1996), *Introduction of Heat Transfer.*, John Wiley & Sons, Inc., New York.
9. MacGregor J. G., (1997), *Reinforced concrete Mechanics and Design*, Third edition, Prentice Hall, Inc., New Jersey, pp.939.
10. Naaman A. E., (2004), *Prestressed Concrete Analysis and Design-Fundamentals*, Techno Press 3000, Michigan, pp.1072.
11. Nowak A.S. (1999). *Calibration of LRFD Bridge Design Code*. NCHRP Report 368, Transportation Research Board, Washington, DC.
12. Nowak A. S. and Rakoczy, Anna M. (2012) "Statistical Resistance Models for R/C Structural Components", *ACI SP-284-6*, Vol. 248, pp. 1–16.
13. Nowak A. S., Collins K. R., (2013), *Reliability of Structures*. CRC Press, New York.
14. Otsuki N., Tadokoro Y., Kojima M., (2010), "Corrosion propagation behavior of stainless steel reinforcement bars in concrete", *Corrosion Engineering journal*. Vol.59, No.45, pp.126–135,
15. Ostermiski K. Schießl P., (2012), "Design model for reinforcement concrete", *Journal of Structural Concrete*, Vol. 13, No. 3, pp.156–165.
16. Samson E. Marchand J., (2007), "Modeling the effect of temperature on ionic transport in cementitious materials" *Cement and Concrete Research* Vol. 37, 455–468.
17. Stewart M.G., (1997), "Time-dependent reliability of existing RC structures", *Journal of Structural Engineering-ASCE*, 123 896–902.
18. Takewaka K., Yamaguchi T., Maeda S., (2003), "Simulation Model for Deterioration of concrete structures due to chloride attack", *Journal of Advanced concrete technology*. Vol.1, No.2, pp.139–146, July.
19. Tanaka Y., Kawano H., Watanabe H., and Nakajo T., (2001), "Study on required cover depth of concrete highway bridges in coastal environment", 17th U.S.-Japan Bridge Engineering Workshop.
20. Thoft-Christensen P. (2008), "Deterioration of Reinforced Concrete Structures", Ikke Angivet, Department of Civil Engineering, Aalborg University.
21. Weng Z.C, Yu H.F., Sun W., Zhang J.H. and Chen H.Y., (2006) "Influence of water-cement ratio and cement content on chloride binding capacity of concrete" *Journal of Wuhan University of Technology*, Vol.28, No.3, pp. 47–50.
22. Williamson G., Weyers R. E., Sprinkel M. M., (2009), "Probabilistic Chloride Corrosion Service Life Model Validation: Global and Individual Bridge Deck Predictions", *Journal of ASTM International*, Vol. 6, No. 9.